

Electron-Phonon Superconductivity in $\text{LaO}_{0.5}\text{F}_{0.5}\text{BiSe}_2$

Yanqing Feng,¹ Hang-Chen Ding,² Yongping Du,¹ Xiangang Wan,^{1*}

Bogen Wang,¹ Sergey Y. Savrasov³ and Chun-Gang Duan^{2,4}

¹*Department of Physics and National Laboratory of Solid State Microstructures, Nanjing University, Nanjing 210093, China*

²*Key Laboratory of Polar Materials and Devices, Ministry of Education, East China Normal University, Shanghai 200062, China*

³*Department of Physics, University of California, Davis, One Shields Avenue, Davis, CA 95616, USA*

⁴*National Laboratory for Infrared Physics, Chinese Academy of Sciences, Shanghai 200083, China*

(Dated: August 26, 2018)

We report density functional calculations of the electronic structure, Fermi surface, phonon spectrum and electron-phonon coupling for newly discovered superconductor $\text{LaO}_{0.5}\text{F}_{0.5}\text{BiSe}_2$. Significant similarity between $\text{LaO}_{0.5}\text{F}_{0.5}\text{BiS}_2$ and $\text{LaO}_{0.5}\text{F}_{0.5}\text{BiSe}_2$ is found, i.e. there is a strong Fermi surface nesting at $(\pi, \pi, 0)$, which results in unstable phonon branches. Combining the frozen phonon total energy calculations and an anharmonic oscillator model, we find that the quantum fluctuation prevents the appearance of static long-range order. The calculation shows that $\text{LaO}_{0.5}\text{F}_{0.5}\text{BiSe}_2$ is highly anisotropic, and same as $\text{LaO}_{0.5}\text{F}_{0.5}\text{BiS}_2$, this compound is also a conventional electron-phonon coupling induced superconductor.

PACS numbers: 74.20.Pq, 74.70.-b, 74.25.Kc

I. INTRODUCTION

In 2012, a new superconductor $\text{Bi}_4\text{O}_4\text{S}_3$ has been found.¹ This material has a layered structure composed of a stacking of rock-salt-type BiS_2 layers and $\text{Bi}_4\text{O}_4(\text{SO}_4)_{1-x}$ blocking layers.¹ The stacking structure of the superconducting and blocking layer is analogous to those of high- T_c cuprates,² and iron pnictides.³ Thus the discovery of $\text{Bi}_4\text{O}_4\text{S}_3$ has immediately triggered a wave of extensive studies.^{1,4-31} In addition to $\text{Bi}_4\text{O}_4\text{S}_3$, several new BiS_2 -based superconductors had been synthesized: $\text{LnO}_{1-x}\text{F}_x\text{BiS}_2$ ($\text{Ln}=\text{La}, \text{Nd}, \text{Ce}, \text{Pr}$ and Yb),⁴⁻⁹ $\text{Sr}_{1-x}\text{La}_x\text{FBiS}_2$ ^{10,11} and $\text{La}_{1-x}\text{M}_x\text{OBiS}_2$ ($M=\text{Ti}, \text{Zr}, \text{Hf}$ and Th).¹² The common feature for these compounds is that they all have the same superconducting BiS_2 layer. Understanding the mediator of pairing as well as the pairing symmetry for this new layered superconductor is therefore a fundamental issue, and attracts a lot of research attention.¹³⁻²⁸

Several theoretical works have been reported, especially for $\text{LaO}_{0.5}\text{F}_{0.5}\text{BiS}_2$,⁴ the compound that possesses the highest T_c among known BiS_2 based materials and whose structure is similar to superconducting iron arsenides $\text{LaFeO}_{1-x}\text{F}_x\text{As}$.³ It has been found that the bands crossing Fermi level are $\text{Bi-}6p$ states and a two p bands electronic model has been proposed based on band structure calculation.¹⁹ Due to the quasi-one-dimensional nature of the conduction bands, a good Fermi-surface nesting with wave vector $\mathbf{k}=(\pi, \pi, 0)$ has been found.¹⁹ The lattice dynamics and electron-phonon interaction of $\text{LaO}_{0.5}\text{F}_{0.5}\text{BiS}_2$ have also been studied using density functional theory based calculations²⁰⁻²². It has been suggested that due to the Fermi surface nesting a charge-density-wave (CDW) instability around M point is essential.²⁰ An ferroelectric-like soft phonon mode have also been proposed.²¹ Basically all

the density-functional linear response calculations give a large electron-phonon coupling constant ($\lambda \sim 0.8$), and suggest $\text{LaO}_{1-x}\text{F}_x\text{BiS}_2$ as a strong electron-phonon coupled conventional superconductor.²⁰⁻²²

In contrast to the band structure calculation, there are also works emphasizing the importance of electron-electron interaction and the possibility of unconventional superconductivity.²³⁻²⁷ Starting from the two-orbital model, the spin/charge fluctuation mediated pairing interactions had been studied by using random-phase approximation,^{23,24} and an extended s -wave or d -wave pairing had been proposed.²⁴ With the assumption that the pairing is rather short range interaction, Liang *et al.* find that the extended s -wave pairing symmetry is very robust.²⁵ Possible triplet pairing and weak topological superconductivity had been suggested based on renormalization-group numerical calculation.²⁶ It had also been proposed that BiS_2 based superconductor possess type-II two-dimensional Van Hove singularities, and the logarithmically divergent density of states may induce unconventional superconductivity.²⁷

There are also debates about the pairing symmetry experimentally. The temperature dependence of magnetic penetration depth have been measured by tunnel diode oscillator technique, and it had been suggested that BiS_2 layered superconductors are conventional s -wave type superconductor with fully developed gap.¹³ Muon-spin spectroscopy measurements (μSR) shows a marked two-dimensional character with a dominant s -wave temperature behavior.¹⁴ On the other hand, both the experimental upper critical field, which exceeds the Pauli limit, and the large ratio $2\Delta/T_c \sim 16.6$ imply that the superconductivity is unconventional.¹⁵ Recently, $\text{NdO}_{1-x}\text{F}_x\text{Bi}_{1-y}\text{S}_2$ single crystals had been grown.^{16,17} Resistivity and magnetic measurements reveal that the superconductivity is really derived from the materials intrinsically.¹⁷ More-

over, a giant superconducting fluctuation and anomalous semiconducting normal state have been found for the single crystal sample, suggesting that the superconductivity in this newly discovered superconductor may not be formatted into the BCS theory¹⁷.

Very recently, a new superconductor $\text{LaO}_{0.5}\text{F}_{0.5}\text{BiSe}_2$ had been discovered.³² $\text{LaO}_{0.5}\text{F}_{0.5}\text{BiSe}_2$ has similar structure of $\text{LaO}_{0.5}\text{F}_{0.5}\text{BiS}_2$ yet with a lower T_c (~ 2.6 K).³² In order to shed light on the superconducting nature of this family, it is essential to investigate $\text{LaO}_{0.5}\text{F}_{0.5}\text{BiSe}_2$. Here we report our theoretical studies of the electronic structure and lattice dynamic properties for $\text{LaO}_{0.5}\text{F}_{0.5}\text{BiSe}_2$. Our first-principles calculation shows that the band structure of $\text{LaO}_{0.5}\text{F}_{0.5}\text{BiSe}_2$ is quite similar as that of $\text{LaO}_{0.5}\text{F}_{0.5}\text{BiS}_2$, there is also a strong Fermi surface nesting at $k = (\pi, \pi, 0)$ (i.e. M point), which leads to imaginary harmonic phonons at this k point associated with in-plane displacements of Se atoms. Although the $\sqrt{2} \times \sqrt{2} \times 1$ supercell frozen phonon calculations confirm a double well related to the soft-mode located at M point, our effective model reveals that the double well is too shallow, consequently the CDW structural phase transition indeed will not happen. Replacing S by Se will reduce the Deybe frequency ω_D as well as the electron-phonon coupling constant λ , which explains the decrease of T_c .

II. COMPUTATIONAL METHOD

Our electronic structure calculations are performed based on the Quantum ESPRESSO package (QE)³³ and ultrasoft pseudopotentials³⁴ and the generalized gradient approximation of Perdew, Burke, and Ernzerhof (PBE).³⁵ The basis set cutoff for the wave functions was 60 Ry while 600 Ry cutoff was used for the charge density. A dense $18 \times 18 \times 6$ k -point mesh had been used in the irreducible Brillouin zone (IBZ) for self-consistent calculations. For structural optimization, the positions of ions were relaxed towards equilibrium until the Hellman-Feynman forces became less than 2 meV/Å. Same as $\text{LaO}_{0.5}\text{F}_{0.5}\text{BiS}_2$,^{20,21} we find that for $\text{LaO}_{0.5}\text{F}_{0.5}\text{BiSe}_2$, spin-orbital coupling (SOC) plays only a marginal role on the electronic states near Fermi level (E_F) and lattice dynamic properties. Thus we neglect it and adopt the scalar relativistic version of QE.³³

III. RESULTS AND DISCUSSIONS

$\text{LaO}_{0.5}\text{F}_{0.5}\text{BiSe}_2$ has a layered crystal structure with a space group $P4/nmm$ ³². This material is formed by alternately stacking of BiSe_2 layers and the blocking layer $\text{Bi}_4\text{O}_4(\text{SO}_4)_{1-x}$. La, Se and Bi locate at $2c$ position, while O/F take the $2a$ site. Being embedded into LaO plane, it had been found that the substitution O by F has only small effect on the BiS_2 layer in $\text{LaO}_{0.5}\text{F}_{0.5}\text{BiS}_2$ ²⁰, and the main influence of F substitution is a carrier

TABLE I: The calculated lattice parameters and Wyckoff positions of $\text{LaO}_{0.5}\text{F}_{0.5}\text{BiSe}_2$. Experimental results are also listed for comparison³².

	Site	Cal.	Exp.
a (Å)		4.1594	4.1753
c (Å)		14.0156	14.2634
z	La ($2c$)	0.0943	0.0947
z	Bi ($2c$)	0.6204	0.6136
z	Se1 ($2c$)	0.3847	0.3933
z	Se2 ($2c$)	0.8115	0.8155

doping²⁰. Thus we simulate $\text{LaO}_{0.5}\text{F}_{0.5}\text{BiSe}_2$ by replacing half of the Oxygen $2a$ -sites by F orderly, despite the substitution may be random in reality. We perform the full structural optimization including the lattice parameters and atomic positions, the optimized lattice parameters and Wyckoff positions are shown in Table I, together with available experimental data³². Our numerical lattice parameters and internal coordinates are in good agreement with the experiment as shown in Table I. For $\text{LaO}_{0.5}\text{Bi}_{0.5}\text{Se}_2$, Bi and Se1 form a nearly perfect plane, while for $\text{LaO}_{0.5}\text{Bi}_{0.5}\text{S}_2$, the experimental and theoretical height of S1 has a large difference^{20,21}, and the importance of buckling of S-atoms have been discussed.²¹

Based on theoretical lattice structure, we perform band structure calculation, and find that the electronic structure of $\text{LaO}_{0.5}\text{Bi}_{0.5}\text{Se}_2$ is similar with that of $\text{LaO}_{0.5}\text{Bi}_{0.5}\text{S}_2$.¹⁹⁻²¹ As shown in Fig.1, the dispersion along Γ to Z line is quite small, clearly implying a two dimensional character of the band structure and the negligible interlayer hybridization. La states, which appear considerably above the E_F , has almost no contribution around E_F . O/F $2p$ states are almost fully occupied and mainly located between -5.0 and -2.0 eV. Hybridized with Bi $6p$ states, Se2 $4p$ states have wider bandwidth, but this state is also located primarily below the E_F , has negligible contribution around the E_F . Bi and Se1 form a layer, consequently these states have strong hybridization. The bands around the E_F basically come from Bi $6p$ with also small contribution from Se1 $4p$ as shown in Fig.1. The density of state at E_F is equal to $N(E_F)=1.97$ eV⁻¹ per unit cell. This corresponds to a bare Sommerfeld specific heat coefficient $\gamma_{bare}=2.42$ mJ/mol K², which is just slightly smaller than the numerical value (~ 3.0 mJ/mol K²) of $\text{LaO}_{0.5}\text{Bi}_{0.5}\text{S}_2$.²² The calculated bare plasma frequencies are $\hbar\omega_{p,xx} = \hbar\omega_{p,yy} = 5.99$ eV and $\hbar\omega_{p,zz} = 0.12$ eV, which corresponds to a very large anisotropy $\sigma_{xx}/\sigma_{zz} \sim 2500$ in the assumption of constant scattering time. This huge anisotropy may be detected via optical or transport measurement for single crystal sample.

We also calculate the Fermi surface and show the results in Fig.2. Very similar to $\text{LaO}_{0.5}\text{F}_{0.5}\text{BiS}_2$,^{19,20} the Fermi surface of $\text{LaO}_{0.5}\text{F}_{0.5}\text{BiSe}_2$ are also two dimensional-like and there is a Fermi surface nesting at wavevector near $\mathbf{k} = (\pi, \pi, 0)$.

Density functional linear response approach has been

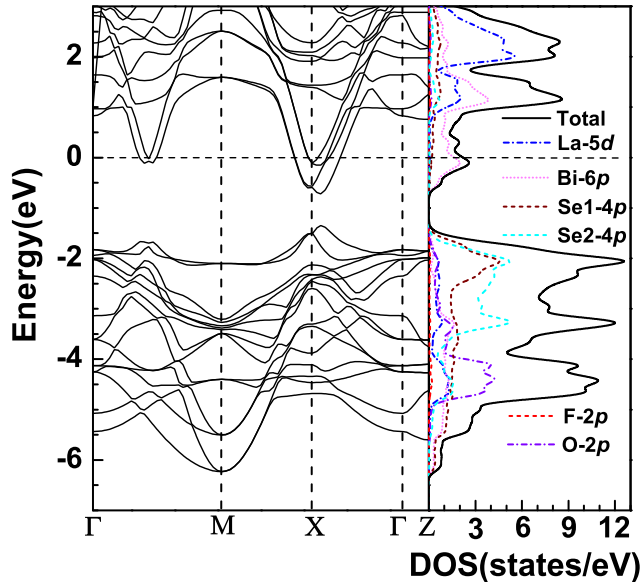


FIG. 1: (Color online) Calculated band structure and density of state of $\text{LaO}_{0.5}\text{F}_{0.5}\text{BiSe}_2$.

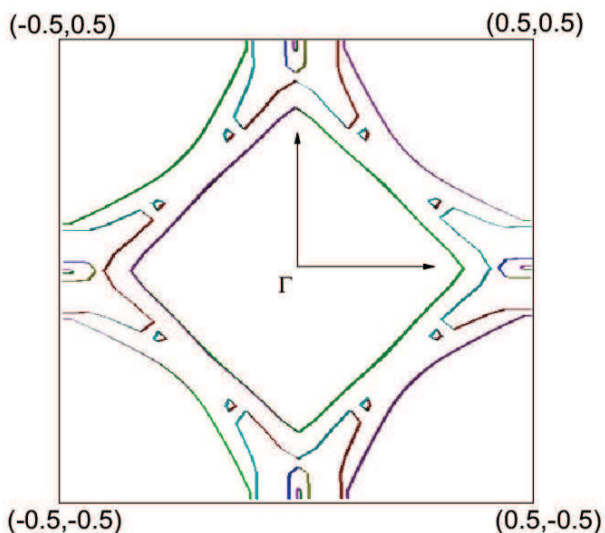


FIG. 2: (Color online) Calculated Fermi surface of $\text{LaO}_{0.5}\text{F}_{0.5}\text{BiSe}_2$: cross section for $k_z=0$.

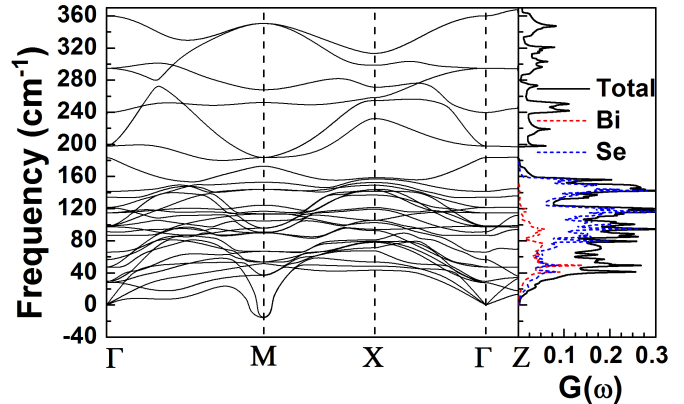


FIG. 3: (Color online) Calculated phonon dispersions and phonon density of state of $\text{LaO}_{0.5}\text{F}_{0.5}\text{BiSe}_2$.

proven to be very successful in the past to describe electron-phonon interactions and superconductivity in metals³⁷, including its applications to Plutonium,³⁸ MgB_2 ,³⁹ and many other systems. Here we apply this first-principles linear response phonon calculation³⁶ as implemented in QE³³ to study $\text{LaO}_{0.5}\text{F}_{0.5}\text{BiSe}_2$. An $18 \times 18 \times 6$ grid was used for the integration over the IBZ. We show the calculated phonon spectrum along major high symmetry lines of the IBZ in Fig.3. Same as $\text{LaO}_{0.5}\text{F}_{0.5}\text{BiS}_2$,²⁰⁻²² the phonon modes have only a little dispersion along Γ -Z direction, which again indicates the smallness of the interlayer coupling. The phonon dispersions are extend up to 350 cm^{-1} , which is smaller than that of $\text{LaO}_{0.5}\text{F}_{0.5}\text{BiS}_2$ ^{20,21}. There are basically two panels in the phonon spectrum. The top six branches above 180 cm^{-1} are almost completely contributed by O and F, while the Bi-Se vibration dominate in the low frequency region. Comparing with $\text{LaO}_{0.5}\text{F}_{0.5}\text{BiS}_2$,²⁰⁻²², $\text{LaO}_{0.5}\text{F}_{0.5}\text{BiSe}_2$ has more branches locate at low frequency region. Analyzing the evolution of the phonon eigenvectors in the IBZ reveals that there is clear separation between the xy and z polarized vibrations, and the phonon modes with large dispersion mainly comes from the Bi-Se1 in-plane vibration.

There are also unstable modes located around M point as shown in Fig.3. We associate it with the strong Fermi surface nesting. The number of soft modes in $\text{LaO}_{0.5}\text{F}_{0.5}\text{BiSe}_2$ is two, while $\text{LaO}_{0.5}\text{F}_{0.5}\text{BiS}_2$ has four unstable modes around M point^{20,21}. From the analysis of the calculated polarization vectors, we find that these two unstable modes are mainly contributed by the Se1 in-plane vibrations.

We then perform a frozen phonon calculation by using a $\sqrt{2} \times \sqrt{2} \times 1$ supercell with respect to its original unit cell to adapt the lattice distortions due to the possible CDW instability associated with the soft phonon mode located at M point. The atomic motions in the frozen phonon

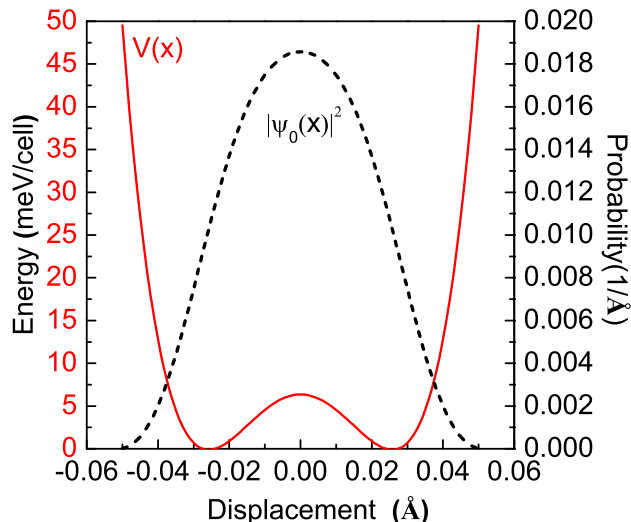


FIG. 4: (Color online) Calculated double well potential (red line) for the unstable phonon mode using the frozen phonon method. The probability plot (black dot line) of the ground state atomic wave function is also shown.

calculation is chosen according to the eigenvectors of the unstable phonon modes at the M point, which basically is Se1 in-plane displacement. The results of these calculations reveal essentially anharmonic interatomic potentials, and a shallow double well potential (~ -6 meV per unit cell) where the Se1 atoms shift about 0.03 Å away from the original high symmetry position as shown in Fig. 4. The depth of the double well is less than half of that in $\text{LaO}_{0.5}\text{F}_{0.5}\text{BiS}_2$.²⁰ For $\text{LaO}_{0.5}\text{F}_{0.5}\text{BiS}_2$ it had been found that the displacements of S atom are dynamic.^{20,21} To check if the quantum zero-point motions also prevent the structural distortion of $\text{LaO}_{0.5}\text{F}_{0.5}\text{BiSe}_2$, we therefore extend the equilibrium position analysis by solving numerically Schrödinger's equation for the anharmonic potential well found from frozen-phonon calculations, as shown in the red line of Fig. 4. Indeed, our numerical atomic ground-state wave function is centered at the high symmetry position, as demonstrated by the probability curve shown in black dot line of Fig. 4. It is therefore clear that the Se1 displacement is dynamic, and the unstable phonon modes at M point are not related to a statically distorted structure of $\text{LaO}_{0.5}\text{F}_{0.5}\text{BiSe}_2$. Experimentally the resistivity changes smoothly from 300 K to about 3 K, and there is not abnormal behavior due to the gap opening associated with CDW phase transition³². This experimental observation is consistent with our above model calculation.

Finally, we check the linewidth $\lambda_\nu(\mathbf{q})$ of all stable phonons to see the contribution from different modes. Calculation shows that the O/F modes have negligible contribution to electron-phonon coupling. With strong hybridization, the coupling, however, is relatively strong for the BiSe based modes. Counting the contribution only from the stable modes results in a coupling constant

($\lambda = 0.47$) calculated using $4 \times 4 \times 2$ q-mesh.

To find the contribution from the anharmonic modes, we follow the expression introduced by Hui and Allen which generalizes zero-temperature electron-phonon coupling to the anharmonic case.⁴⁰ We make an essential approximation by assuming that the unstable mode is not coupled to the other modes. The phonon-phonon interactions and finite-temperature effects are also neglected in this treatment. Basically we need all phonon excited states.^{40,41} Fortunately, it had been found the convergency in the sum over the virtual phonon states is fast.^{40,41} By taking the harmonic dipole matrix elements, and interpreting the first excitation energy from solving the Schrödinger's equation for the anharmonic atomic potential well as the phonon energy,⁴⁰ we estimate the electron-phonon coupling for the two anharmonic modes at the M point. Our numerical λ value from this two modes is about 0.04. Adding this value with the contribution from all stable modes gives us a total coupling constant of 0.51, which is about half of that of $\text{LaO}_{0.5}\text{F}_{0.5}\text{BiS}_2$.²⁰ The estimated Deybe temperature ($\omega_D = 220$ K) is also smaller than that of $\text{LaO}_{0.5}\text{F}_{0.5}\text{BiS}_2$.²⁰ With these values and taking the Coulomb parameter $\mu^* \simeq 0.1$, McMillan formula yields values of $T_c \simeq 2.40$ K in reasonable agreement with the experiment.³²

IV. CONCLUSIONS

We have studied the electronic structure, lattice dynamics and electron-phonon interaction of the newly found superconductor $\text{LaO}_{0.5}\text{F}_{0.5}\text{BiSe}_2$ using density functional theory and linear response approach. Same as in the case of its cousin $\text{LaO}_{0.5}\text{F}_{0.5}\text{BiS}_2$, a strong Fermi surface nesting is also found at $(\pi, \pi, 0)$, which results in phonon softening, and we find that the quantum fluctuation prevents the appearance of static long-range order. Considering both harmonic and anharmonic contributions to electron-phonon coupling, we obtain a coupling constant $\lambda \sim 0.51$, which is capable of producing the experimental T_c value and suggesting $\text{LaO}_{0.5}\text{F}_{0.5}\text{BiSe}_2$ as an electron-phonon superconductor.

Acknowledgments

X.G.W acknowledges useful conversations with Prof. H.H. Wen, J.X. Li, Q.H. Wang, Donglai Feng and Dawei Shen. This work was supported by the National Key Project for Basic Research of China (Grants No. 2011CB922101, 2010CB923404, 2013CB922301 and 2014CB921104), NSFC under Grants No. 91122035, 11174124, 11374137, 61125403), PAPD, Program of Shanghai Subject Chief Scientist, PCSIRT. Computations were performed at the ECNU computing center.

*xgwan@nju.edu.cn

-
- ¹ Y. Mizuguchi, H. Fujihisa, Y. Gotoh, K. Suzuki, H. Usui, K. Kuroki, S. Demura, Y. Takano, H. Izawa and O. Miura, *Phys. Rev. B* **86**, 220510 (2012).
- ² W. E. Pickett, *Rev. Mod. Phys.* **61**, 433 (1989).
- ³ Y. Kamihara, T. Watanabe, M. Hirano, and Hideo Hosono, *J. Am. Chem. Soc.* **130**, 3296 (2008).
- ⁴ Y. Mizuguchi, S. Demura, K. Deguchi, Y. Takano, H. Fujihisa, Y. Gotoh, H. Izawa and O. Miura, *J. Phys. Soc. Jpn.* **81** 114725 (2012).
- ⁵ S. Demura, Y. Mizuguchi, K. Deguchi, H. Okazaki, H. Hara, T. Watanabe, S. J. Denholme, M. Fujioka, T. Ozaki, H. Fujihisa, Y. Gotoh, O. Miura, T. Yamaguchi, H. Takeya and Y. Takano, *J. Phys. Soc. Jpn.*, **82**, 033708(2013).
- ⁶ S. Li, H. Yang, J. Tao, X. Ding and H. H. Wen, *Phys. Rev. B* **86**, 214518 (2012).
- ⁷ V. P. S. Awana, A. Kumar, R. Jha, S. Kumar, J. Kumar, A. Pal, Shruti, J. Saha, S. Patnaik, *Solid State Commun.* **157**, 31 (2013); R. Jha, H. Kishan, and V. P. S. Awana, *J. Appl. Phys.* **115**, 013902 (2014).
- ⁸ R. Jha, A. Kumar, S. K. Singh, V. P. S. Awana, *J. Sup. and Novel Mag.* **26**, 499 (2013); R. Jha, A. Kumar, S. K. Singh, V.P.S. Awana, *J. Appl. Phys.* **113**, 056102 (2013).
- ⁹ D. Yazici, K. Huang, B. D. White, A. H. Chang, A. J. Friedman, M. B. Maple, *Philosophical Magazine* **93**, 673 (2012).
- ¹⁰ X. Lin, X. Ni, B. Chen, X. Xu, X. Yang, J. Dai, Y. Li, X. Yang, Y. Luo, Q. Tao, G. Cao, Z. Xu, *Phys. Rev. B* **87**, 020504 (2013).
- ¹¹ H. Lei, K. Wang, M. Abeykoon, E. S. Bozin, C. Petrovic, *Inorg. Chem.* **52**, 10685 (2013).
- ¹² D. Yazici, K. Huang, B. D. White, I. Jeon, V. W. Burnett, A. J. Friedman, I. K. Lum, M. Nallaiyan, S. Spagna, and M. B. Maple, *Phys. Rev. B* **87**, 174512 (2013).
- ¹³ Shruti, P. Srivastava and S. Patnaik, *J. Phys.: Condens. Matter* **25** 312202 (2013).
- ¹⁴ G. Lamura, T. Shiroka, P. Bonf, S. Sanna, R. De Renzi, C. Baines, H. Luetkens, J. Kajitani, Y. Mizuguchi, O. Miura, K. Deguchi, S. Demura, Y. Takano, and M. Putti, *Phys. Rev. B* **88**, 180509 (2013).
- ¹⁵ S. Li, H. Yang, D. Fang, Z. Wang, J. Tao, X. Ding, H.-H. Wen, *Sci. China-Phys. Mech. Astron.* **56**, 2019 (2013).
- ¹⁶ M. Nagao, S. Demura, K. Deguchi, A. Miura, S. Watauchi, T. Takei, Y. Takano, N. Kumada, I. Tanaka, *J. Phys. Soc. Jpn.*, **82**, 113701, (2013).
- ¹⁷ J. Liu, D. Fang, Z. Wang, J. Xing, Z. Du, X. Zhu, H. Yang, H.-H. Wen, arXiv:1310.0377 (2013).
- ¹⁸ J. Lee, M. B. Stone, A. Huq, T. Yildirim, G. Ehlers, Y. Mizuguchi, O. Miura, Y. Takano, K. Deguchi, S. Demura, and S.-H. Lee, *Phys. Rev. B* **87**, 205134 (2013).
- ¹⁹ H. Usui, K. Suzuki and K. Kuroki, *Phys. Rev. B* **86**, 220501 (2012).
- ²⁰ X. Wan, H.-C. Ding, S. Y. Savrasov, C.-G. Duan, *Phys. Rev. B* **87**, 115124 (2013).
- ²¹ T. Yildirim, *Phys. Rev. B* **87**, 020506 (2013).
- ²² B. Li, Z. W. Xing and G. Q. Huang, *EPL* **101**, 47002 (2013).
- ²³ T. Zhou and Z. D. Wang, *J. Superconductivity and Novel Magnetism* **26**, 2735 (2013).
- ²⁴ G. B. Martins, A. Moreo, and E. Dagotto, *Phys. Rev. B* **87**, 081102 (2013).
- ²⁵ Y. Liang, X. Wu, W.-F. Tsai, J. P. Hu, arXiv:1211.5435 (2013).
- ²⁶ Y. Yang, W.-S. Wang, Y.-Y. Xiang, Z.-Z. Li, and Q.-H. Wang, *Phys. Rev. B* **88**, 094519 (2013).
- ²⁷ H. Yao, F. Yang, arXiv:1312.0077 (2013).
- ²⁸ S.L. Liu, *J. Supercond. Nov. Magn.* **26**, 3411 (2013).
- ²⁹ S. K. Singh, A. Kumar, B. Gahtori, Shruti, G. Sharma, S. Patnaik, V. P. S. Awana, *J. Am. Chem. Soc.* **134**, 16504 (2012).
- ³⁰ S. G. Tan, L. J. Li, Y. Liu, P. Tong, B. C. Zhao, W. J. Lu, Y. P. Sun, *Physica C*, **483**, 94 (2012).
- ³¹ R. Jha, V. P. S. Awana, arXiv:1311.0161 (2013).
- ³² A. Krzton-Maziopa, Z. Guguchia, E. Pomjakushina, V. Pomjakushin, R. Khasanov, H. Luetkens, P.K. Biswas, A. Amato, H. Keller, K. Conder, arXiv:1310.8131 (2013).
- ³³ *Quantum-ESPRESSO* is a community project for high-quality quantum-simulation software, based on density-functional theory, and coordinated by Paolo Giannozzi. See <http://www.quantum-espresso.org>
- ³⁴ D. Vanderbilt, *Phys. Rev. B* **41**, 7892 (1990).
- ³⁵ J. P. Perdew, K. Burke, and M. Ernzerhof, *Phys. Rev. Lett.* **77**, 3865 (1996).
- ³⁶ S. Baroni, S. de Gironcoli, A. Dal Corso, and P. Giannozzi, *Rev. Mod. Phys.* **73**, 515 (2001).
- ³⁷ S. Y. Savrasov and D. Y. Savrasov, *Phys. Rev. B* **54**, 16487 (1996).
- ³⁸ X. Dai, S. Y. Savrasov, G. Kotliar, A. Migliori, H. Ledbetter, E. Abrahams, *Science* **300**, 953 (2003).
- ³⁹ Y. Kong, O. V. Dolgov, O. Jepsen, and O. K. Andersen, *Phys. Rev. B* **64**, 020501 (2001).
- ⁴⁰ J.C.K. Hui, and P.B. Allen, *J. Phys. F: Met. Phys.* **4**, L42 (1974).
- ⁴¹ V. Mereghalli and S. Y. Savrasov, *Phys. Rev. B* **57**, 14453 (1998).